

# THE 1.8 TESLA, 4.8 M I.D. BUBBLE CHAMBER MAGNET\*

J.R. Purcell  
Argonne National Laboratory  
Argonne, Illinois

## INTRODUCTION

The 1.8 T\*\* magnetic field for the ANL 3.7 m chamber (Fig. 1) is provided by energizing coils (Fig. 2) wound from copper-clad, Nb48%Ti strip (Fig. 4) and immersed in liquid helium at 4.5°K (1.2 bar†) contained in a toroidal stainless-steel reservoir. The 4.8 m i.d. coils are located in a carbon steel yoke which forms a low reluctance return path for the magnetic flux. The use of iron reduces the ampere-turns needed to produce the required magnetic field. The carbon steel yoke and heavily copper-clad superconductor were chosen to give a reliable conservative magnet. The coil and cryostat are cooled by a separate closed cycle liquid helium refrigeration plant. A conventional power supply is used to energize the coil which is protected by low resistance, room temperature resistors. These can be switched across the coil terminals when required. The 3000 A, 10 V dc power supply is adequate to charge the magnet to design current in 2.5 hours.

The operating cost of the coil should be \$400 000/year less than an equivalent copper coil because of the saving in electrical power. A conventional electromagnet of this performance with copper coils would have the same capital cost as the supermagnet (\$3 000 000). It may be possible to replace the present coil with a 4.0 T coil which has the same winding space at some future date. The principal characteristics of the magnet are given in Table I.

The arrangement of the superconducting coils within the iron yoke and bubble chamber system is shown in Fig. 3. The inner and outer vacuum cans, and intermediate radiation shield can be seen in more detail in Fig. 4, where their position with respect to the windings is shown. The use of iron with a simple rectangular coil section results in a high field uniformity over the chamber volume (15%). Stray magnetic fields are reduced by the iron which also provides a sturdy mechanical foundation for the whole structure. The major portion of the frame is made up of castings weighing up to about 100 t.‡ Eddy current heating in the moving parts of the bubble chamber system is low because the field uniformity is high. This reduces the production of heat in the moving parts of the expander system and consequently the heat load on the hydrogen refrigeration system.

## ENERGIZING COIL SYSTEM

The coil structure is split into two sections (Figs. 1, 3, and 4) to permit the beam of high energy particles to enter the chamber in a plane perpendicular to the line

---

\* Reprinted from Argonne National Laboratory Report ANL/HEP 6811 (1968), edited by C. Laverick.

\*\* 1 T = 10 kG.

† 1 bar = 0.99 atm = 100 000 N/m<sup>2</sup>.

‡ 1 t = 1000 kg.

TABLE I

Superconducting Magnet Characteristics

Operating current at 1.8 T central field	2200 A
Ampere turns (30 pancakes of 84 turns each)	$5.5 \times 10^6$
Inductance at windings	40 H
Field uniformity over working volume	$\pm 2.5\%$
Current density in conductor	$1700 \text{ A/cm}^2$
Average current density in windings	$775 \text{ A/cm}^2$
Energy stored in field	$80 \times 10^6 \text{ J}$
Weight of copper in windings	45 000 kg
Weight of superconductor	300 to 400 kg
Coil axial compressive force	$6.8 \times 10^5 \text{ kg}$
Compressive stress on coil separators	$140 \text{ kg/cm}^2$
Outward force between coil halves	450 000 kg
Weight of iron	$1.45 \times 10^6 \text{ kg}$
Inside diameter of coil	478 cm
Outside diameter of coil	528 cm
Length of coil	304 cm
Power supply voltage	10 V
Charging time	2.25 h
Heat transfer rate required for 100% stability	$0.13 \text{ W/cm}^2$
Resistance/cm of conductor copper at 2.0 T field and 4.2°K	$1.32 \times 10^{-8} \text{ } \Omega/\text{cm}$
Total winding resistance at 4.2°K and 2.0 T assuming superconductor completely normal	0.031 $\Omega$
Total power dissipation at 2200 A (no superconductor)	150 kW

of sight of the cameras which are located on top of the system. The coil system and cryostat weigh 45 t each. They are hung from the magnet yoke by pairs of stainless-steel pipes of total cross-sectional area  $690 \text{ cm}^2$  spaced at  $90^\circ$  to each other. The complete support system can accommodate a vertical load of 450 t. The tension in the central connector ring during operation is 450 t since each coil half is attracted to its adjacent pole piece when the coil is energized. The coil system is centered magnetically with respect to the iron. If displaced it could experience a force of 20 t/cm of vertical displacement which increases in direct proportion to its distance from the equilibrium position.

Similarly the constant for lateral displacement is 14 t/cm. The maximum lateral force is 45 t and the lateral support structure is designed to withstand 225 t. This lateral support structure consists of two sets of four 7.95 cm diameter, 1.5 m long titanium rods spaced at  $90^\circ$  to each other which connect the top and bottom 10 cm thick stainless-steel girder rings in the winding structure to the iron return frame. The

heat leak to the helium bath from the magnet iron through the lateral support rods is limited to 50 W by wrapping each rod with gas cooling tubes and flowing 50°K helium gas through the tubes to intercept the incoming heat.

The enclosing vacuum vessel of the cryostat is fabricated from 2.5 cm thick type 503 aluminum and is designed in accordance with Section VIII of the ASME Unfired Pressure Vessel Code for an external pressure of 1.01 bar and an internal pressure of 1.38 bar. It has a 25 cm diameter emergency vent which is activated at 1.38 bar. This vessel acts as a short-circuited turn around the magnet with an 8 sec time constant. This is considerably longer than the 0.25 sec time constant for the helium can so that most of the coil energy on fast discharge will be absorbed by the external coil circuit and this can. The two beam access windows in the cryostat are spaced 90° to each other with an aperture of 18 cm x 68°. Aluminized Mylar multilaminar insulation is used in conjunction with an aluminum radiation shield.

Each coil half comprising 15 pancake units is divided into two coil sections each of which has its own liquid helium container (Figs. 2 and 4). This is accomplished by fitting annular stainless-steel vessels over each coil section and welding them to the central support rings (see Fig. 5). These rings serve as the primary support and alignment reference for the complete coil structure and contain suitable interconnections for the liquid helium chambers so as to form a single helium reservoir for the coil structure. The diameter of the helium can structure will shrink 1.5 cm during cooldown from 300°K to 4.2°K so the vertical and radial support systems are arranged to accommodate this contraction. Each of the four liquid helium containers is provided with an inlet and outlet gas manifold and interconnecting holes permit access for current leads, instrumentation leads and emergency helium ejection if necessary. The venting system and helium vessel pressure ratings (4.5 bar) are adequate to support a 200 kW power dissipation inside the helium reservoirs if necessary although it is difficult to see how this can occur. The wall thickness of the helium vessels at the inner diameter is 2.5 cm and at the outer diameter is 1.5 cm while the normal internal operating pressure will be 1.2 bar.

Eight spirally wound pancake units are assembled in the lower section and seven in the upper section to comprise the 15 pancake 2.8 m high stack of each coil half. The spacing between each coil half is 51 cm. The pancakes of each coil stack are assembled with spacer blocks between them covering only a small fraction of the total cooling surface area. These pancake stacks are then tied together by rods welded to the stainless-steel rings on either side of the stack. The assembly is shown in Fig. 5 where the arrangement of the pancakes with respect to the containing vessels is shown. The top ring of the top coil half and the bottom ring of the bottom coil half are actually the top and bottom, respectively, of the helium Dewar vessel. The interpancake electrical connections consisting of double sections of the stabilized conductor are attached to the i.d. and o.d. turns of the pancakes to form a series circuit. The winding ends and the jumper leads are anchored mechanically to prevent any motion and stressing of these electrical joints. The coil terminal leads are treated in the same manner. These details are obvious from Fig. 6 in which the mode of clamping of the coil stacks to the girder ring with stainless-steel tie rods is shown as are the spacer blocks, thermal clamps, pancake interconnections and conductor clamps.

The 60 spacers located between adjacent pancakes at 6° intervals are epoxy-coated aluminum having a cross section of 5 cm x 1.25 cm thick. They extend beyond the i.d. and o.d. when installed. Each section is capped with a set of spacers and a clamp plate. The clamp plates are connected to the central girder rings via 2.2 cm diameter threaded aluminum rods. There are 60 rods on the i.d. and 60 rods on the o.d. The aluminum rods are screwed to the clamp plate, but pass through holes in the girder ring. They are prestressed to approximately 276 bar via nuts which bear against the

girder ring. The 0.45 cm differential contraction between the pancake structure and girder ring diameters on cooldown is taken up by incorporating a sliding interface at the junction between the two.

A section through the copper-clad six-strand Nb48%Ti conductor is shown in Fig. 7 and its principal characteristics are tabulated below. In operation the conductor is edge-cooled in static liquid helium at 4.5°K.

TABLE II  
Conductor Specification 4.8 m i.d. Argonne  
Bubble Chamber Magnet

Width	5.0 cm
Thickness	0.25 cm
Individual piece length	220 m
Individual piece weight	240 kg
Critical characteristics, field parallel to strip cross section	a) 3000 A at 2.5 T - specified b) 4000 A at 2.5 T - measured
Critical characteristics, field normal to strip cross section	3000 A at 1.35 T - specified
Calculated stable current	4300 A at 2.5 T
Calculated recovery current	3300 A at 2.5 T
Resistance ratio of copper cladding $\rho(273^{\circ}\text{K})/\rho(4.2^{\circ}\text{K})$	200
Design stress	840 kg/cm <sup>2</sup>
Percentages of copper and superconductor in strip	96% Cu, 4% Nb48%Ti in six separate strands
Resistance/cm of conductor at 4.2°K and 2 T	$1.32 \times 10^{-8} \Omega$
Area of strip/cm length of conductor exposed to helium bath	0.5 cm <sup>2</sup>
Estimated heat transfer rate from exposed conductor surface for 0.1°K temperature rise in conductor	0.13 W/cm <sup>2</sup>
Operating current at 1.8 T central field	2200 A

The measured performance of the conductor exceeded its specified performance by more than 30% (Table II). The edge-cooled pancakes will operate in the stable mode if necessary with a heat dissipation of 0.13 W/cm<sup>2</sup> of exposed conductor surface for a 0.1°K temperature rise in the conductor. The cryogenic system is adequate for such a heat load. The strip contains sufficient copper to support the hoop stresses generated during magnet operation. The design characteristics for the strip were further checked by cutting each of the first three lengths delivered in half and winding them to form a six pancake coil of 60 cm i.d., 85 cm o.d., and 38 cm height. The total winding length was 690 m and the coil weight was 800 kg. Teflon tape and epoxy formed the

interturn insulation and bond. When tested the coil carried 4600 A while developing maximum fields of 3 T parallel and 1.9 T normal to the strip cross section and it was the 1.9 T condition which caused the transition in the superconductor. Current sharing between the copper and superconductor began at 4650 A which exceeds the minimum acceptable specifications of Table II by a large margin, thus providing an ample reservoir of performance stability. This test coil is shown in Fig. 8.

#### THERMAL PROBLEMS ON COOLDOWN

One of the major design problems in using such large structures at low temperatures is that of minimizing thermal stress. The large diameter of the magnet makes it very sensitive to thermal stress. Vertical thermal gradients produce a shear load on the bond between turns within the coils. Keeping the total vertical temperature differential,  $\Delta T$  to less than  $10^{\circ}\text{K}$  will limit this shear stress to less than 140 bar. Laboratory tests have shown that this type of bond has a shear strength of from 210 to 700 bar. Temperature gradients are no problem during operation of the magnet because it is at a uniform temperature of  $4.5^{\circ}\text{K}$ . The thermal gradient problem occurs only during cooldown or on accidental discharge of the magnet and must be considered over the range from  $300^{\circ}\text{K}$  down to about  $50^{\circ}\text{K}$ . Below this temperature, thermal expansion coefficients are so small that thermal stress is not a problem. In order to limit the  $\Delta T$  to  $10^{\circ}\text{K}$ , the cold gas used for cooling is introduced into each coil compartment through a manifold that extends completely around the circumference of the coils. This manifold has small holes spaced about every 6 in. to spray the cold gas downward and mix it with the warm gas within the container. Initially, liquid nitrogen will be used to cool this incoming gas so the inlet temperature will be about  $80^{\circ}\text{K}$ . The helium refrigerator compressor will be used to circulate this gas during cooldown. The gas is returned to the compressor through another  $360^{\circ}$  manifold at the bottom of each coil package. Introducing the cooling gas in this manner sets up convection currents within each coil compartment resulting in a very large mass flow of gas. The average temperature of this large gas flow is only slightly below that of the coils resulting in a uniform coil temperature. A second method of improving temperature uniformity is thermally shorting the ends of the aluminum spacer blocks together. This is done with a heavy copper braid and is shown in Figs. 2, 6, and 9.

The design philosophy was checked by constructing a model similar to the test coil using only copper strip. The thermal clamps chosen to equalize temperatures throughout the larger structure were used in this model which is shown in Fig. 9. The technique chosen for bonding the turns together was also used in this model. The mechanical integrity of the structure when subjected to several successive thermal shocks by cycling its temperature from  $77^{\circ}\text{K}$  to room temperature was found to be adequate.

#### COIL FABRICATION

A single pancake is shown in Fig. 10 in position on its winding jig in ANL after completion of the winding process. The coils were wound in a horizontal plane to permit easy access to the pancake during winding. The winding line consisted of an initial splicing and inspection station followed by cleaning and tensioning equipment and then the 6 m diameter winding fixture. The Teflon insulation was fed through an epoxy roll coater and guided onto the winding fixture about  $30^{\circ}$  ahead of the point where the conductor was fed in. Six lengths of the 210 m long pieces supplied were connected together by using 30 cm long, lead tin soldered, copper rivetted lap joints between successive lengths to form the continuous single lengths required for each pancake. Abrasive brushes were used to remove burrs from the conductor which was sand-blasted and then washed with alcohol to provide a good keying surface for the interturn epoxy bonding material.

The combination of the thin layer of brittle epoxy adhesive with a comparatively thick layer of flexible insulating sheet as interturn insulation was chosen to permit some shearing to take place without breaking the brittle bond. The flexible fluorinated ethylene-propylene insulation was etched prior to application of the epoxy to provide a better bonding surface.

The degree of flatness and accuracy of winding thickness for the pancakes was assured by hand grinding using an appropriate fixture. This was necessary for accurate and rigid assembly of the final coil stack. All pancakes were tested for turn-to-turn electrical short circuits to ensure their freedom from such defects before installation in the final stacks. When one section of a 15 pancake half coil assembly had been stacked and clamped to the girder rings, the entire structure was turned over and the other portion was stacked and clamped to form the complete package shown in Fig. 2. The assembly with all its leads, connectors, and instrumentation was then fully inspected and tested before the helium cans were welded into place on the girder ring.

#### COIL STACK TEST PROCEDURES

The following tests were made to ensure correct assembly of the magnet and to provide information for future maintenance.

The actual location of the windings with reference to the girder ring was determined at 90° intervals to  $\pm 0.075$  cm. The entire assembly was carefully cleaned and inspected. All parts were checked for mechanical integrity. All log books, drawings, and records were reviewed to ascertain that every component had been installed according to design.

The coil stack was energized at room temperature to 15 A at 39 V and turn-to-turn voltage drop measurements were carried out and recorded. The voltages at all potential taps were recorded to check their potential tap location. All instrumentation leads were checked for continuity, resistance, isolation, etc. (as applicable). The resistances between the coils and support structures were measured. A check was made to ensure that there were no shorts or possible shorts which could arise from magnetic forces on unsupported current-carrying elements.

A field profile at the i.d. of the windings was made at the approximate location of the i.d. of the helium can, and the vacuum can. All internal structures were inspected to determine the existence of closed electrical loops which could interact with a time changing field. The winding sense of the coil structure was noted and the external leads were marked appropriately.

#### MAGNET YOKE AND SUPPORT STRUCTURE

Constraints on the yoke design included its large size, the means of absorbing the pulsating expander forces, accommodating the coil and cryostat structure, and integrating the complete system. Cyclic operation of the expander system generates inertial forces equivalent to the weight of the magnet iron (1360 t). Restrictions on the basic design and fabrication techniques with such a large structure are imposed by available manufacturing facilities. Shipping and material handling capacities limit the size of individual pieces.

Lateral forces on the windings are minimized by making the iron structure symmetrical about its central axis. There are no forces on the windings when they are magnetically centered. The requirement for two beam access windows of 2.4 m azimuthal width located at 90° with respect to one another, coupled with the need for cylindrical

symmetry in the iron structure, dictated that there be four 2.4 m windows equally spaced (90°) in the median plane. Low reluctance return paths and high field uniformity are achieved with the geometry used for this yoke. The magnet poles form the top and bottom of the hydrogen chamber vacuum can. Accidental liquid hydrogen leakage can be contained by the aluminum cryostat vacuum can around the hydrogen chamber and vacuum wall.

The magnet iron consists of top plate and bottom plate assemblies, each 7.6 m<sup>2</sup> by 1.27 m separated by four corner posts at a distance of 3 m. The top and bottom plate assemblies each contain 500 t of steel in eight pieces ranging in weight from 15 to 100 t. The return legs contain 600 t of steel in eight identical pieces (two 75 t pieces in each of the four corners). The principal estimated loads on the top and bottom magnet blocks are given in Table III.

TABLE III  
Estimated Magnet Block Loads

Induced vacuum loading on top and bottom core blocks	154 t
Outward loading on top and bottom core blocks due to 11 bar vacuum can test pressure	1540 t
Bottom core loading due to chamber operation	
a) At 12 bar maximum operating pressure	1260 t
b) At 15.8 bar maximum test pressure	1530 t
Due to limitation of pressure differential across the omega bellows to 4 bar	
a) At 8.3 bar operating pressure on piston bottom	1090 t
b) At 11.7 bar test pressure on piston bottom	1540 t
Due to 4 bar cyclic pressure	220 (constant) ± 220 (cyclic) t downwards
Maximum circular deflections at the vacuum can sealing surfaces on the more highly stressed bottom core blocks	0.06 cm
Weight of each bottom core block piece	100 t

The maximum allowable impurities for the magnet iron as shown by a ladle analysis are: carbon - 0.20, silicon - 0.05, manganese - 0.80, sulphur - 0.05, phosphorous - 0.05, and aluminum - 0.05. The minimum allowable yield and tensile strengths for the highly stressed core blocks are 2000 and 4000 bar, respectively. The remaining parts of the yoke have minimum yield and tensile strengths of 1300 and 2600 bar, respectively. Minor surface and internal imperfections are tolerated in most portions of the yoke so long as they do not impair the gross mechanical integrity of the piece.

Tolerances on individual pieces were chosen to give a mechanically sound structure. Shimming was allowed provided that the shim at any joint covers the entire

mating surface area and is of uniform thickness over that area. Localized imperfections were tolerated along mating surfaces if they did not degrade the structural integrity. Repair welding was allowed anywhere. Tolerances on unmachined and external surfaces were chosen to minimize cost. Small imperfections were tolerated on all machined surfaces except the pole piece vacuum seals. Alignment pins, dowels, handling holes, bosses, and lifting eyes were permitted in the iron wherever they did not interfere with system assembly. These simplify repeated construction and breakdown. The complete iron structure was assembled at the vendor's plant prior to breakdown into separate pieces for shipment.

#### POWER SUPPLY AND ENERGIZING COIL SYSTEM

The power supply is a three-phase, full wave, thyristor controlled unit whose time average output voltage can be varied by adjusting the firing angle of the thyristors. It is equipped with the usual safety interlocks and fault indicating lamps. These circuits include a holding circuit so that the appropriate lamp has to be reset manually to energize the power supply when a fault has been cleared. Provisions have been made for a remote permissive interlock to operate in conjunction with the relay contacts of the fault indicator. This contact interlock in the bubble chamber control room should be closed before the power supply can be energized.

The magnet windings are protected against a sudden release of the stored magnetic energy if for some reason the coil begins to discharge quickly. A possibility would be a sudden increase in coil resistance due to the liquid helium level dropping below the top of the coil and the subsequent loss of cooling. Two means of protection are provided. The first method consists of a "dump resistor" (Fig. 11) which is always in the electrical circuit, connected in parallel with the coil. Should a resistive region develop in the coil, both the power supply and the stabilizer resistors will be disconnected from the circuit and the coil current will flow through the dump resistor. The energy stored in the magnetic field will then be dissipated in the dump resistor at an initial rate of approximately 0.4 MW (2000 A at 200 V for designed operating conditions). Even in the worst case, with the whole coil being resistive, at least 60% of the energy will be dissipated in the dump resistor. The second protective measure guards against pressure buildup in the helium vessel and high local temperature rise in a resistive coil region. At a preset pressure rise in the Dewar (caused by helium vaporization in the proximity of the power dissipating region), the bulk of the liquid helium can be rapidly transferred from the Dewar to a dump tank. With the helium removed, the whole coil will become normal and power will be uniformly dissipated throughout the windings. If the full stored magnetic energy of 80 MJ and 1.8 T is absorbed by the total thermal mass of the windings, the coil temperature will rise only to about 90°K. Since the liquid helium has been removed from the tank, the temperature rise of the coil will not result in any serious pressure rise of the system.

The emergency dump resistor is a 0.1  $\Omega$ , grounded center tap, large thermal mass resistor. A heavy duty, double pole switch is located close to and on the power supply side of this resistor. When this switch is opened, the magnet current (and field) will decay with a time constant of approximately 6.6 min. Under normal conditions, the dump resistor will absorb very nearly the total energy stored in the system. If the magnet windings were to become completely resistive, the dump resistor would absorb approximately 60% of the total stored energy. It contains approximately 942.5 kg of No. 1008 carbon steel strip wound in 10 pancakes connected in series parallel to give the correct resistance. Its temperature rise with 100 MJ input and no cooling would be 250°C. The dump resistor value was selected to limit the peak voltage across the system to approximately 300 V dc. The energy dump switch interrupts both power leads to the magnet (double pole, single throw). The switch is designed to interrupt a maximum magnet current of 3000 A dc.

The dump system will be tested at incrementally increasing current levels during initial system checkout. A  $0.2 \Omega$  (grounded center tap) resistor and an automatically operated power supply output shorting switch are connected across the power supply bus on the power supply side of the dump switch. The former will protect the power supply from high voltage transients during dump switching and the latter will protect the water-cooled free-wheeling diode in the event of loss of cooling.

A schematic diagram of the power supply circuit is given in Fig. 12. The frequency response from the input of the thyristor control unit to the output of the power supply should be 7 Hz minimum. The power supply, free-wheeling diode, and fast discharge resistor are all water-cooled. Protection against flow failure and component overheating is provided. The shunt resistors across the magnet limit the peak voltage to less than 600 V during all discharge conditions. Manual reversing links are provided so that the current flow in the magnet may be reversed if required.

The voltage regulated supply has its reference derived from the error signal between the magnet current and a reference. The purpose of the voltage loop is to remove any power line induced voltage variations and also to linearize the voltage control. The voltage loop, which consists of the differential amplifier  $A_2$ , a ripple filter, and the amplifier  $A_1$ , has an open loop gain of 100. The operator may select either the voltage or current regulation mode by a switch on the front panel of the power supply. When operated in the voltage regulate mode, the supply voltage is set by a front panel control. When the power supply is operated in the current regulate mode, the operator may set the charge rate of the power supply by a front panel control.

Current control is provided by a circuit which compares the current read by the precision current transducer to the reference voltage. When the error voltage into the temperature stabilized amplifier  $A_3$  exceeds approximately 80  $\mu\text{V}$  (0.004% at 2000 A) the relay  $K_1$  will operate which switches the input to  $A_1$  to either the charge rate reference or to ground (0 volts). The reference voltage for  $A_3$  is derived from a temperature regulated zener diode and a stabilized buffer amplifier. Control of the reference voltage is by a four-position thumbwheel switch which permits a resolution of  $10^{-4}$  in setting the magnet current. The variation of the supply current and coil voltage with current during operation is shown in Fig. 13. The necessary degree of field stability is maintained with this on-off control because of the large inductance and high stored energy of the magnet. The basic accuracy of the current readout transducer is 0.1% at 2000 A. The accuracy will degrade to about 2% at currents below 500 A. The output from the transducer is used as the feedback voltage for the regulator and for external use.

The normal current decay of the power supply is set by the forward voltage drop across the free-wheeling diodes and the voltage drop in the dc bus which connects the magnet to the power supply. For a 0.5 V drop in the diodes, the decay rate is  $13.2 \times 10^{-3}$  A/sec. The fast discharge resistor has been provided to increase the current decay to 0.250 A/sec. This is a manually triggered operation. The return to the normal current decay rate is automatic when the magnet current reaches the value preset on the current reference. The anticipated long-term current deviations are as tabulated below:

- 1) Current reference -  $24.8 \times 10^{-6}$  V/ $^{\circ}\text{C}$ .
- 2) Current sensing amplifier -  $0.1 \times 10^{-6}$  V/ $^{\circ}\text{C}$ .
- 3) Current transducer -  $34 \times 10^{-6}$  V/ $^{\circ}\text{C}$ , based on a  $10^{-3}$  V/A.

Based on a temperature variation of  $\pm 5^{\circ}\text{C}$ , a total error of  $\pm 29.4 \times 10^{-6}$  V is predicted. This is equivalent to  $\pm 0.015\%$  at 2000 A.

The safety circuits are designed to protect the magnet in the event of a power failure. If the cooling system fails or the power supply overheats the primary voltage is removed from the rectifier transformer, and the output shorting switch is closed. The shorting switch around the fast discharge resistor will be closed if it overheats and the power supply will continue to operate normally. The magnet is protected by meter relays against overvoltage (either polarity) and overcurrent. The meters, which are located on the control panel of the power supply, have a visible trip point which is manually adjustable from the front of the meter.

#### HELIUM REFRIGERATOR

The performance characteristics and main load for the helium refrigerator are given in Table IV. The refrigerator is also used to cool the superconducting coils and containers from ambient temperature to liquid helium temperature. When used in this fashion the full compressor flow is taken through the exchangers and then to the cooldown distribution header of the magnet. Warm helium vapor is removed from the magnet can and returned to the compressor section after this gas has passed through a heater. The helium refrigerator has to maintain the superconducting magnet of the 3.7 m bubble chamber at a temperature of 4.5°K for continuous and indefinite periods of time. High reliability with periods of downtime kept to short duration is the primary requirement for the refrigerator.

TABLE IV

Load Characteristics for the Helium Refrigerator

Performance characteristics under:

- a) Normal operation with liquid hydrogen precooling.
- b) Modified operation with liquid nitrogen and a second expansion engine in place of the hydrogen stage.

Cooling for insulation shield around the magnet reservoir	500 W at 50°K - normal 500 W at 80°K - modified
Maintenance of liquid in storage and magnet Dewar	400 W at 4.45°K - normal 320 W at 4.45°K - modified
Counterflow cooling of power supply leads and supports	25 liquid liter/h of helium - normal and modified

Liquid hydrogen is available in large quantities in this bubble chamber complex and is also generated by a hydrogen refrigerator of large capacity so liquid hydrogen precooling is used. An expansion engine in parallel with the J-T (Joule-Thomson) expansion valve is used to lower the capital investment in the plant and to give high reliability. The expansion engine can be removed and installed without interruption of refrigerator operation. The helium refrigeration system can be used to cool the magnet and its container from ambient to operating temperature. Liquid nitrogen and liquid hydrogen can be used for cooling the magnet to decrease the time required for cooldown.

A second expansion engine can be used instead of liquid hydrogen precooling to provide refrigeration at times when liquid hydrogen is not desired in the bubble chamber building. A substantial storage capability for liquid helium is provided. Vacuum-jacketed transfer lines which can be replaced in a short period of time without need

For purging or evacuation are incorporated. The cold box of the refrigerator is divided into two parts so that equipment containing hydrogen liquid and vapor can be placed in a separate enclosure containing an inert atmosphere. This ensures greater safety. The system uses components of proven capability.

The helium refrigerator together with the liquid storage Dewar (11 000 liter capacity, including 1000 liters of ullage volume), and the superconducting magnet can (6500 liter volume) constitute a closed system. Ignoring leakage, gas and liquid is kept in the system for an indefinite period of time. Gas can be stored in a vessel, which has a capacity of 2100 m<sup>3</sup>.

The rate of liquid vaporization may temporarily exceed the capacity of the refrigerator. During this time, excess gas is compressed by the compressor and put in the gas storage vessel. When excess gas is present, the suction pressure of the compressor will increase and the compressor will automatically handle more gas. Gas will be drawn from the vessel when the rate of liquefaction exceeds the rate of liquid vaporization. This occurs automatically since the suction pressure of the compressor is then reduced. The helium refrigerator system will operate automatically without attendance. The compressor requires occasional blowdown of oil knockout drums. The helium purification system requires occasional reactivation (once every 24-48 hours, depending on level of contamination). Except for these two operations, the system will operate and adjust itself to upsets in the form of more or less demand for refrigeration. The automatic operation is achieved by means of pressure and liquid level sensors. Pressure sensors will automatically monitor and maintain the suction pressure of the compressor. It may happen that the compressor discharge pressure will decay, but this will only be a result of excess refrigeration capacity and a depleted gas storage vessel.

The instrumentation necessary for checkout and operation of the helium refrigerator is concentrated in two areas. Compressor operation with its pressure and temperature indicators, controllers and alarms is located in the compressor room. Cold box instrumentation is divided between the compressor room and a panel located near the helium-helium cold box. The refrigerator system is operated from the compressor room so that information required during normal operation of the system is available in the compressor room. This information is supplemented with information available at the helium-helium cold box. The local information is useful during the initial checkout of the refrigeration system. As an example, all temperature and some pressure data are needed to assess the heat exchanger performance, but once these have been checked out, abnormal conditions will be indicated by the pressure readouts in the compressor room.

#### PRINCIPAL PERFORMANCE PARAMETERS - HELIUM REFRIGERATOR

The three main parameters which determine the performance of the refrigerator are, the heat transfer, insulation, and expander efficiencies, assuming the compressor operation to be satisfactory.

The heat exchangers have been designed to perform with a predetermined temperature difference between the high and low pressure helium streams. When the low pressure gas does not reach its design temperature at the warm end of the heat exchangers, the high pressure gas becomes too warm at the cold end of the exchanger. This causes a large deterioration in heat exchanger performance, e.g. a 1<sup>o</sup>K increase in high pressure gas temperature at the cold end of Exchanger III represents a loss of 200 W of refrigeration. Temperature sensors are provided for both low and high pressure gas streams at both ends of the exchangers to allow an assessment of heat exchanger performance to be made at any time.

Loss of insulation of the high vacuum from 0.013 to 13 or 130 ubar will represent a loss of several hundred watts of refrigeration. All vacua except those in the

transfer lines are monitored by vacuum gauges, but it is easy to detect poor vacua by sensing outside vacuum wall temperatures of the equipment. Heat is supplied from the air to the wall at an approximate rate of  $5000 \text{ J/h}\cdot\text{m}^2$  for each  $1^\circ\text{C}$  of temperature difference.

The total amount of refrigeration provided at the  $4.5^\circ\text{K}$  temperature level is divided between J-T effect and expander work. Under normal operating conditions, the J-T effect accounts for one-third and the expander for two-thirds of the total refrigeration. The contribution of the J-T effect is easily determined from a measurement of the temperatures of the gas at the warm end of Exchanger III. The contributions of the expander inlet and outlet temperatures are approximately the same. The expander is equipped with the means to observe P-V diagrams which permit evaluation of the machine performance. This evaluation should always begin with a check of the thermal, insulation, and expander efficiencies and the compressor performance.

### SAFETY CONSIDERATIONS

The sealing surface at the lower magnet pole is subject to cyclic deflection as a result of expander loading. Although the core blocks are rectangular, the deflection contours at this radius are approximately circular. All deflections are small and there will be no degradation of the "O" ring seals. These seals are protected against rupture due to a hydrogen spill by suitable heaters, flow deflectors, and superinsulation. The system is designed to permit an overpressure due to a hydrogen spill into the vacuum space of 11.376 bar, above which it will be automatically vented to the atmosphere. It will also withstand a pressure of 1.01 bar in the vacuum space and in vacuum between the chamber bottom plate and the piston which could occur due to operator error. The vacuum vessel and its beam window are protected from external damage by the cryostat vacuum can which forms a capsule around that entire system.

This yoke is designed to withstand all the magnetic, pressure and vacuum, and expander system loads. The bolting procedures for the upper and lower core blocks have been clearly specified by prevent failure due to improper bolting. The iron structure can withstand any reasonably anticipated hydrogen spill without cracking. The bottom plate assembly components are subject to fatigue. They will be inspected carefully during initial repeated cooldowns to  $77^\circ\text{K}$  and routinely inspected during normal operation.

The most critical hazards are those which could change the over-all force distribution on the winding structure. Interlocks are provided to prevent the magnet from being energized without the top and bottom poles and core blocks in place. Forces on all coil support members are routinely monitored and checked. Coil hoop stresses and clamping tie bar stresses are monitored using strain gauges. The design stress values can be exceeded by a large margin without hazard.

Connectors and leads will withstand all anticipated magnetic forces and thermal motions. Voltage taps are located across each joint and connection so that possible failures can be detected. Coil temperatures are monitored to limit thermal stresses during cooldown. The major effects of thermal stresses would be loss of the turn-to-turn bond in the winding pancakes and pancake-to-spacer bonds which should not affect operation. An alarm will indicate a low helium level condition. Such a condition should not damage the winding structure. All windings have been carefully tested to ascertain that there are no shorts at installation. Strainers have been installed at the helium systems to keep short-causing chips and debris to a minimum. Any shorts in the windings during a field transient could redistribute the currents and hence the magnetic forces. The energy will be dumped at a low field level each time the magnet is turned on to determine the vertical forces on the winding support structure and assess if any significant change has taken place.

If the field decay rate is dominated by the vacuum can, the stresses induced in the can may cause the aluminum to yield but not break. The can is securely locked into place in the iron so that it cannot move during such a field transient. It also serves as a protective capsule around the hydrogen chamber and its vacuum wall and can withstand and vent hydrogen spills due to simultaneous failure of the beam windows in both the hydrogen chamber and the hydrogen chamber vacuum wall. The vacuum can is adequately vented to accept helium vessel failure. Low vacuum in the can will actuate an alarm but the vacuum space also has a radiation shield and superinsulation so that in the event of vacuum failure, both the heat leak and resulting pressure rise in the helium bath will be relatively slow.

The helium refrigeration system provides adequate liquid helium storage to permit eight hours of magnet system operation without the refrigerator. This should allow adequate time for normal maintenance and emergency repair of the refrigeration system if necessary.

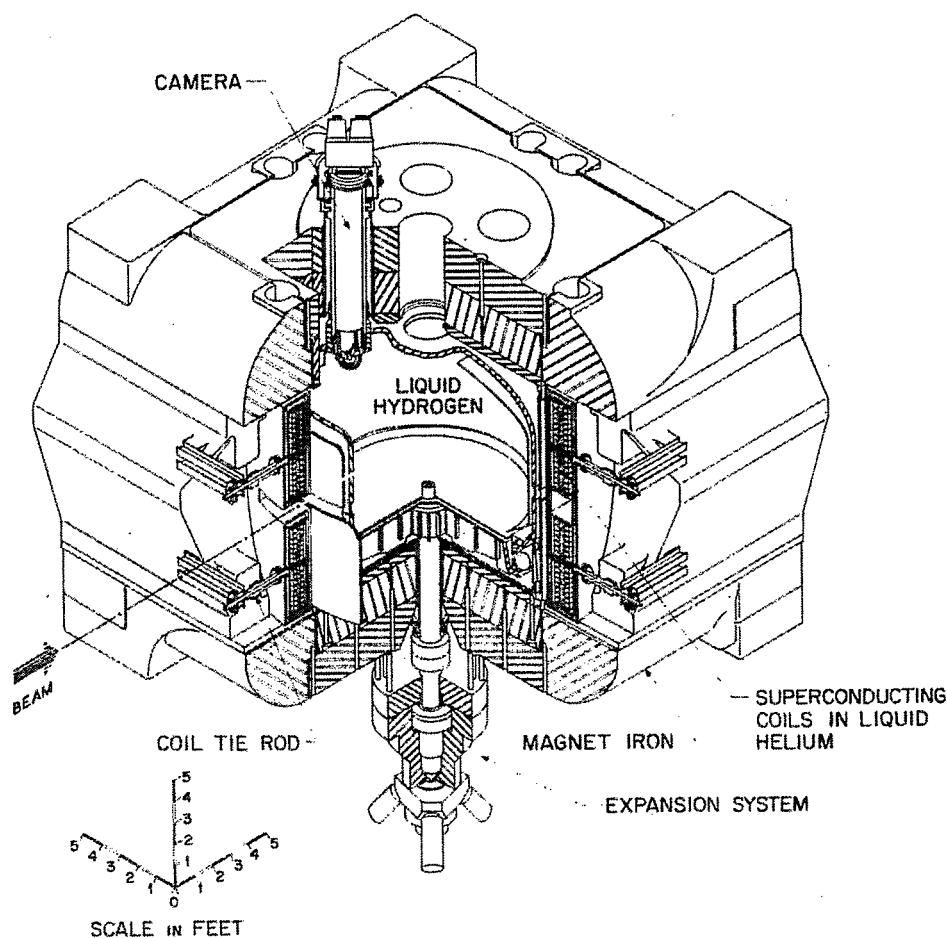


Fig. 1. Over-all view of the ANL 3.7 m hydrogen bubble chamber showing the location of the chamber, expansion system, coil assembly and cryostat with respect to the iron yoke and particle beam access window.

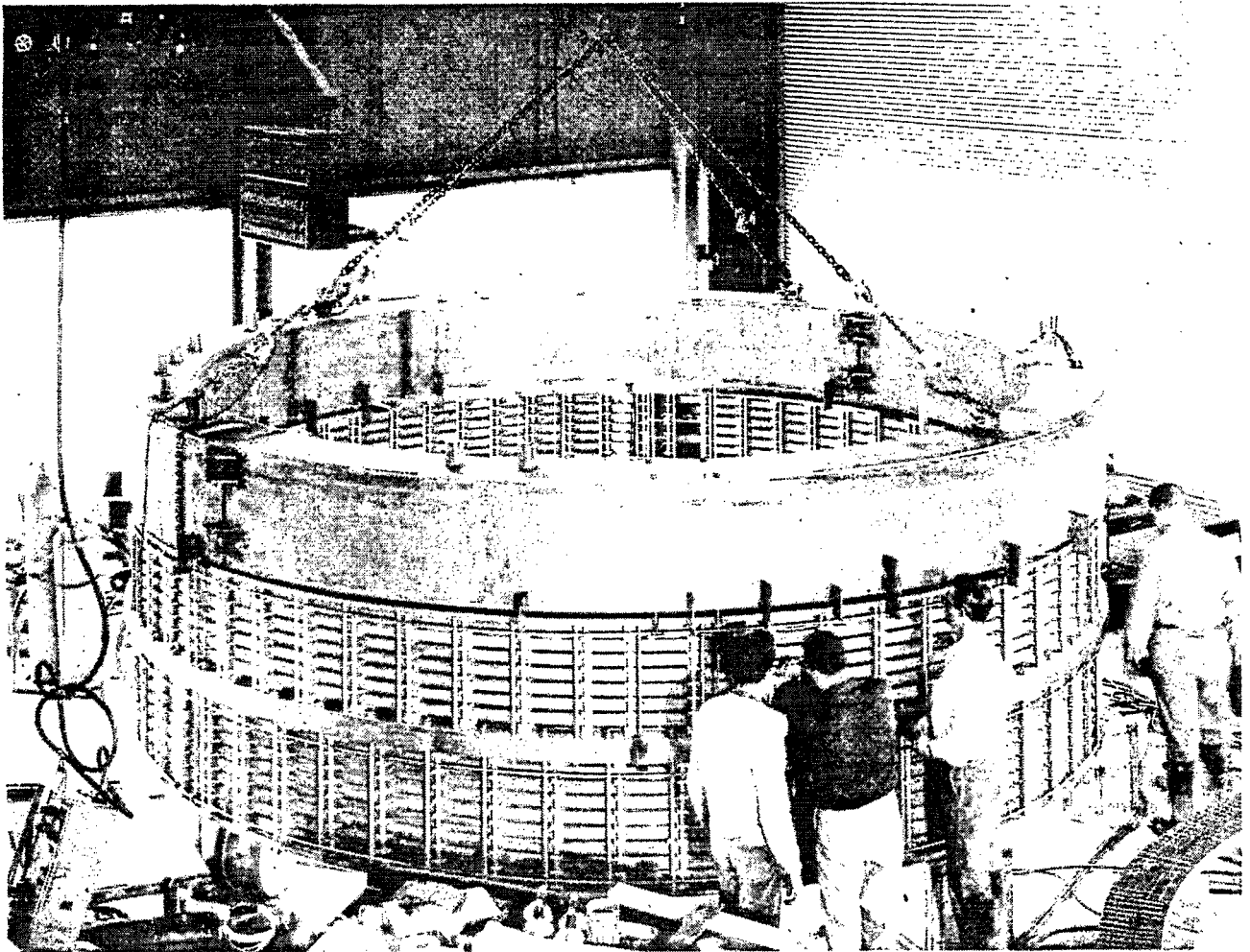


Fig. 2. One of the two 4.8 m i.d. coil halves of the 1.8 T hydrogen bubble chamber magnet showing details of the 15 pancake assembly. The vertical braided copper thermal interconnections between separate pancake units minimize temperature differentials and hence thermal stresses during cooldown. A section of the stainless-steel helium can is shown suspended above the assembly. This can forms the vacuum tank for the magnet.

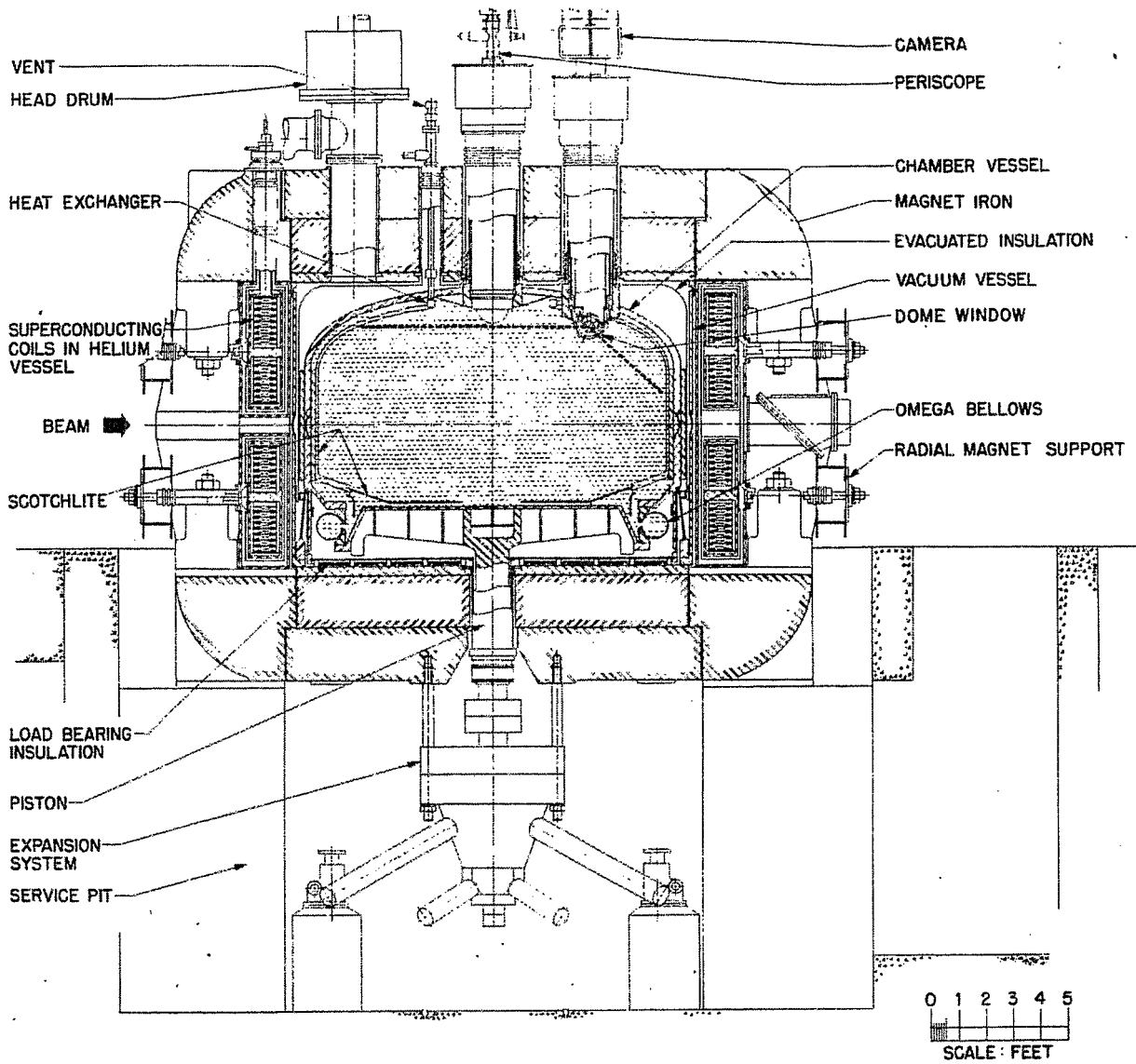


Fig. 3. A cross section through the ANL 3.7 m hydrogen bubble chamber system.

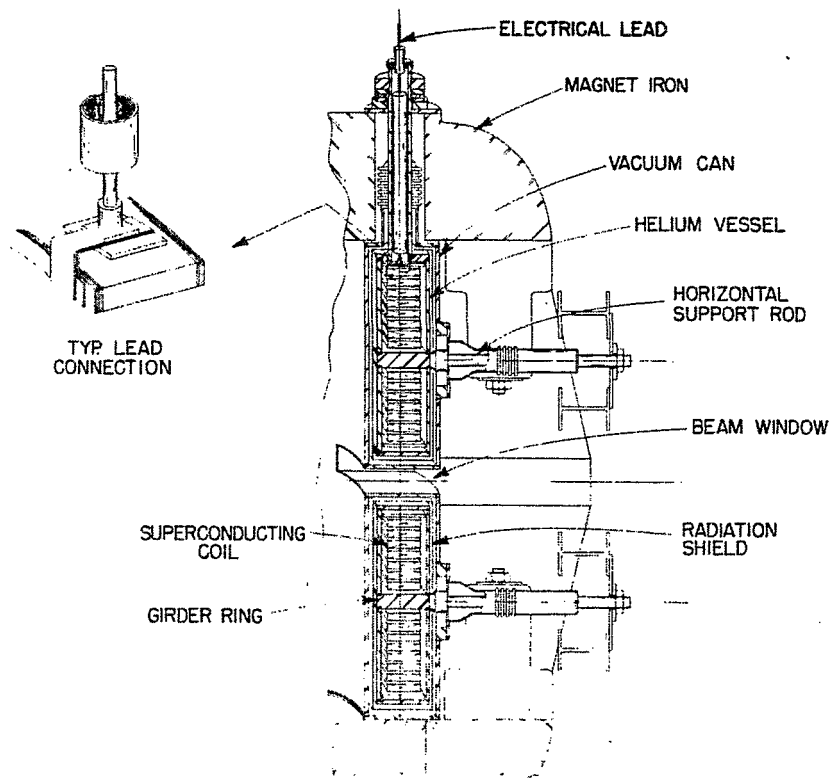


Fig. 4. Schematic of a portion of the magnet cross section showing the location of the coil assemblies in the helium vessel and vacuum enclosure, their respective locations and the support structure.

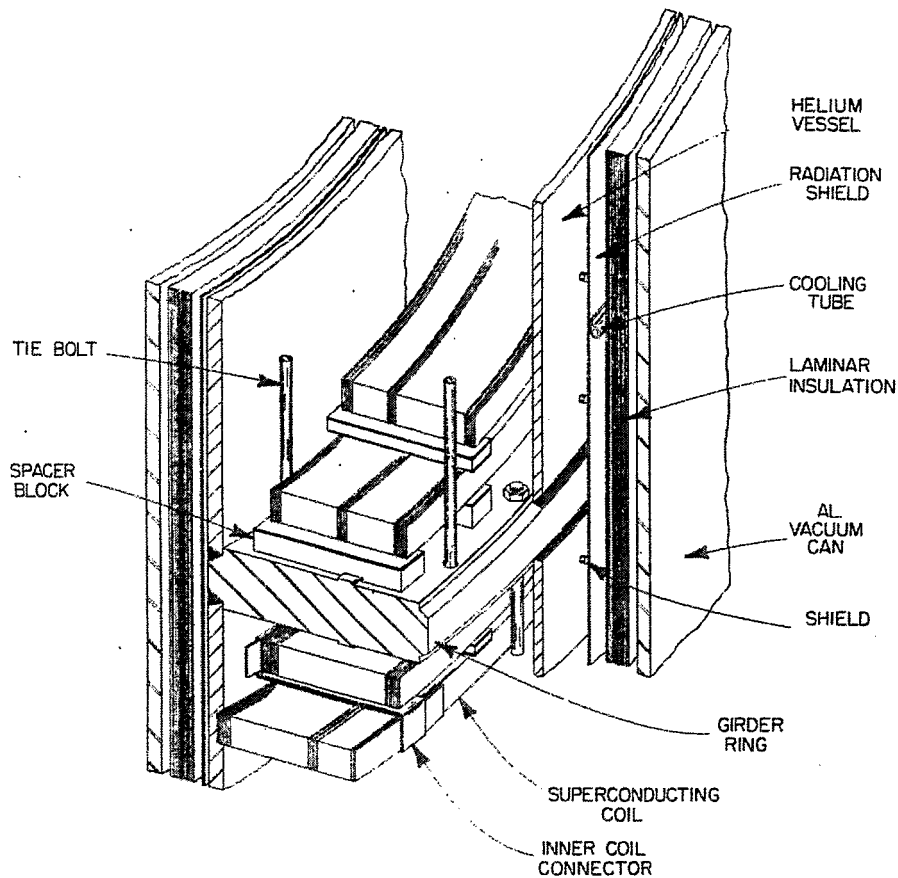


Fig. 5. Detail showing the arrangement of the individual pancakes with respect to the containing vessels, the mode of connection of the internal girder rings to the helium vessel, the type of electrical interconnections between pancakes and the spacer block arrangement between pancakes.

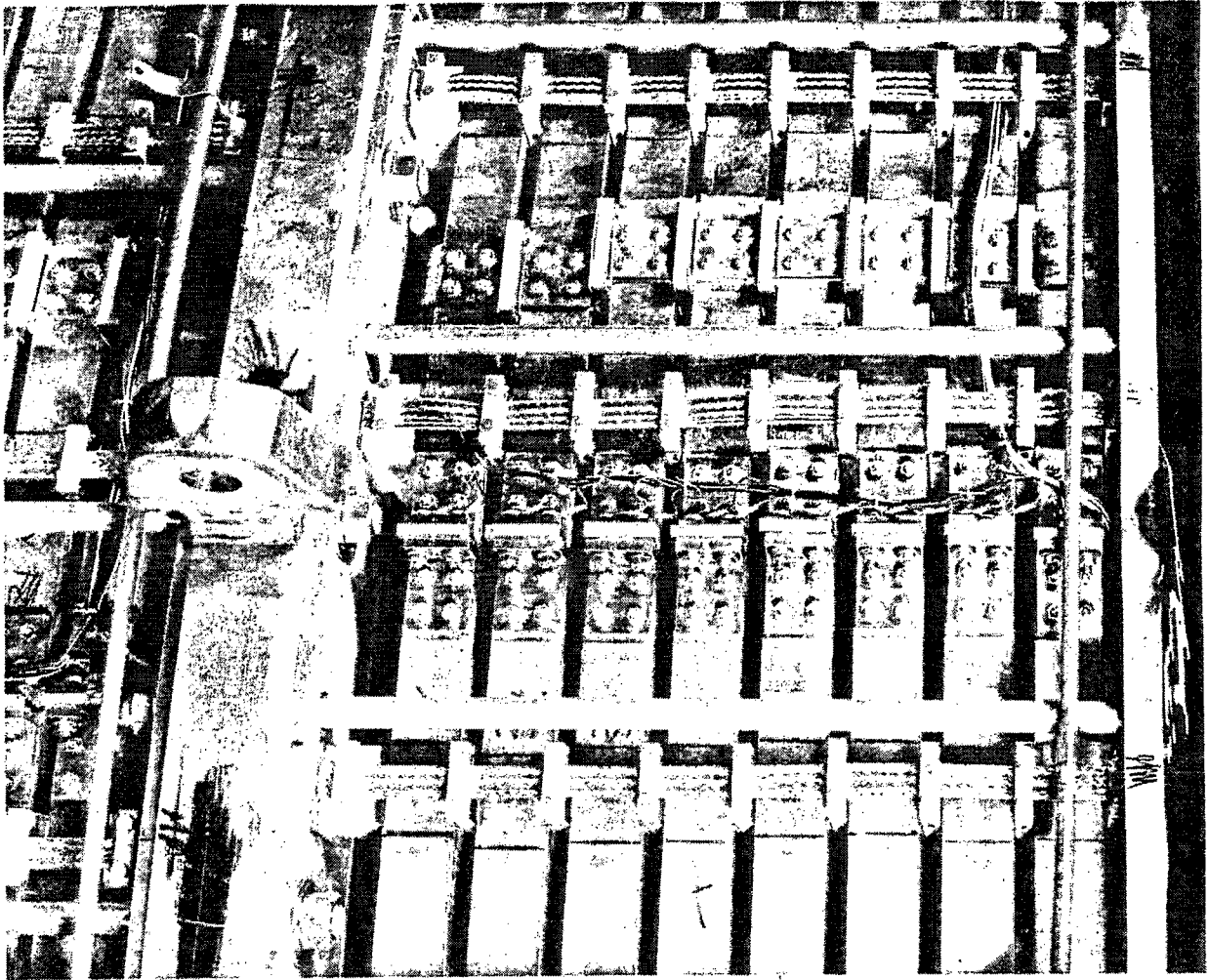


Fig. 6. Photograph of a portion of a coil assembly showing the mode of clamping of a coil stack to the girder ring with stainless-steel tie bolts, the thermal clamps, the electrical interconnections between pancakes and the mechanical clamping arrangement for the ends of the conductor.

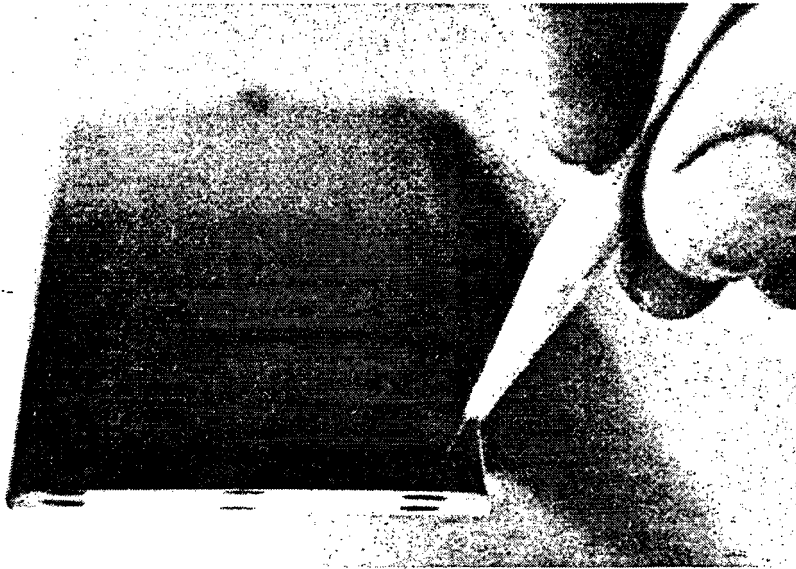


Fig. 7. A cross section of the copper-clad six-strand Nb48%Ti conductor for the 1.8 T, 4.8 m i.d. hydrogen bubble chamber magnet.

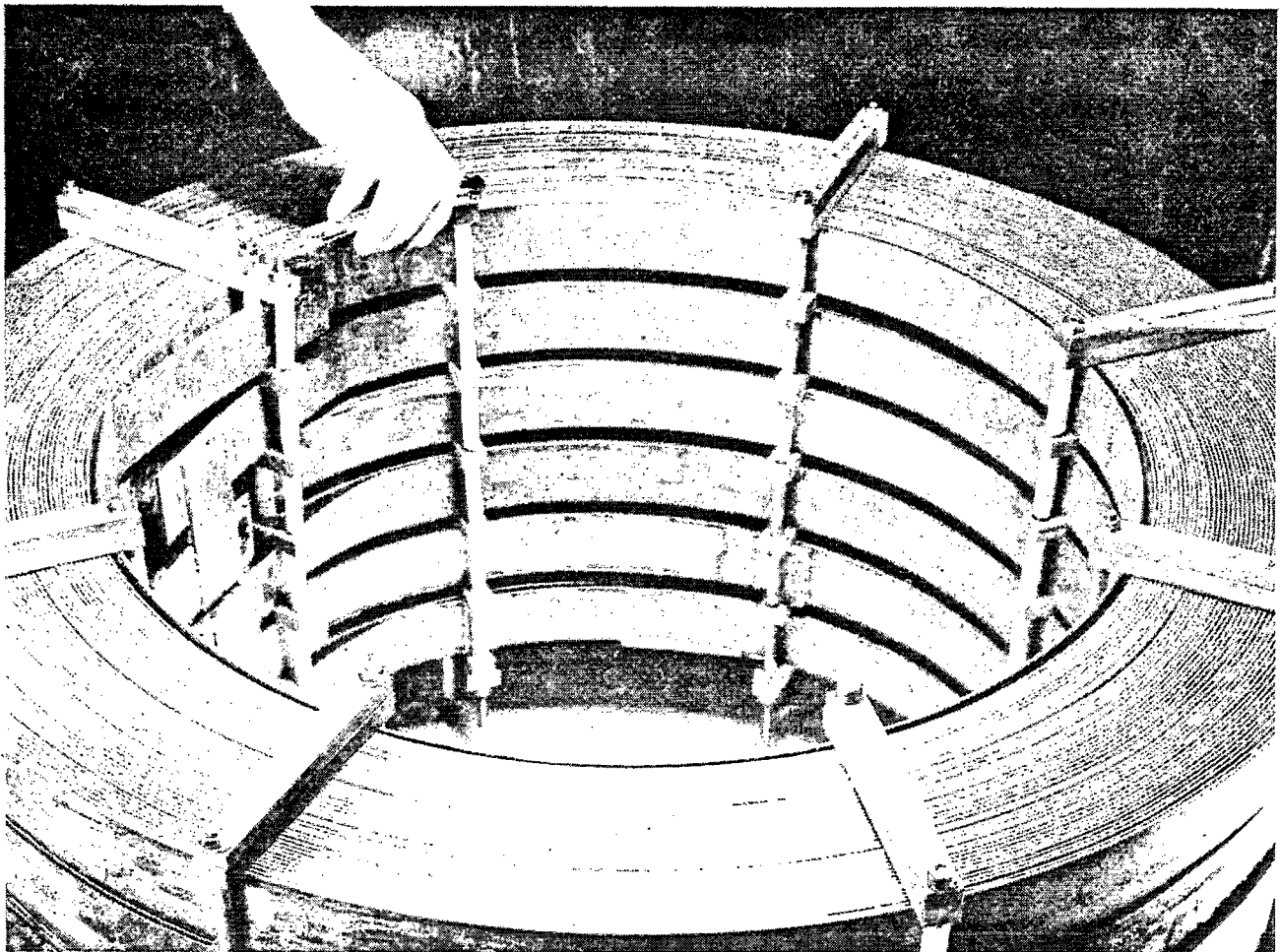


Fig. 8. A six pancake, 4600 A, 2.5 T test coil using the first three lengths of composite strip supplied for the large hydrogen bubble chamber magnet project.

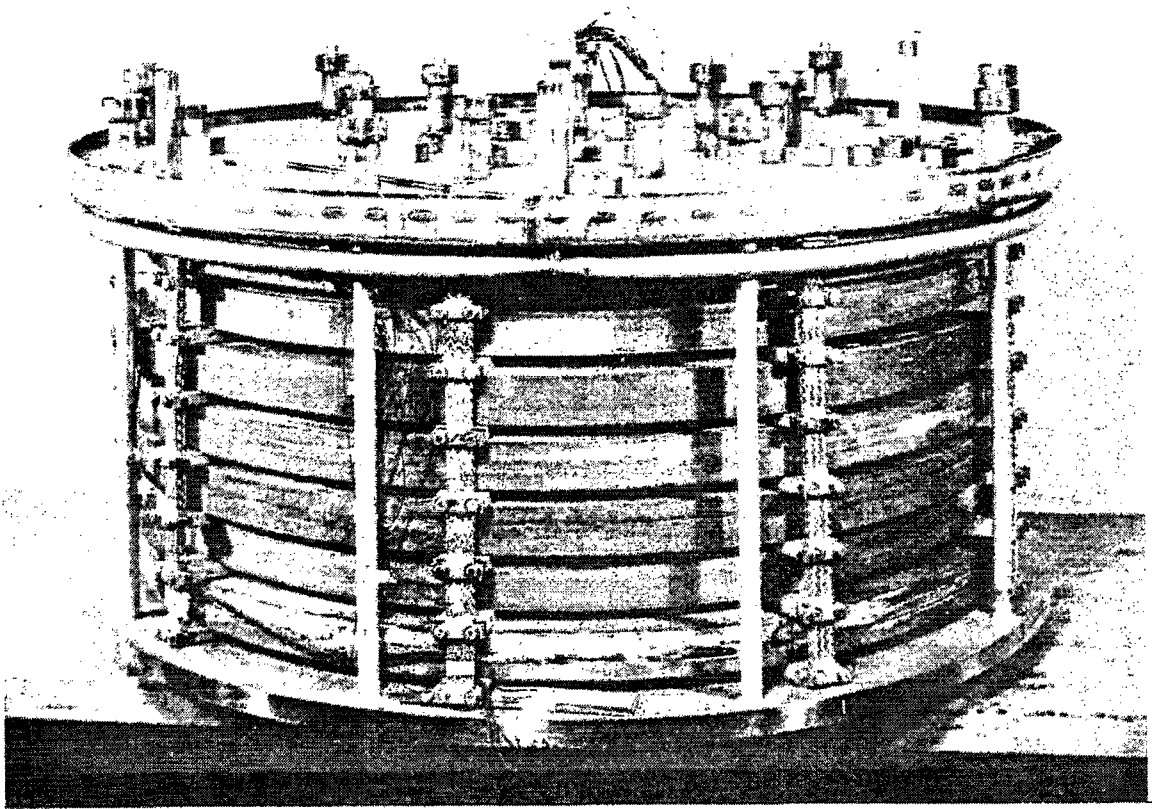


Fig. 9. Cooldown test model to check the efficiency of the design from the point of view of minimizing thermal stresses.

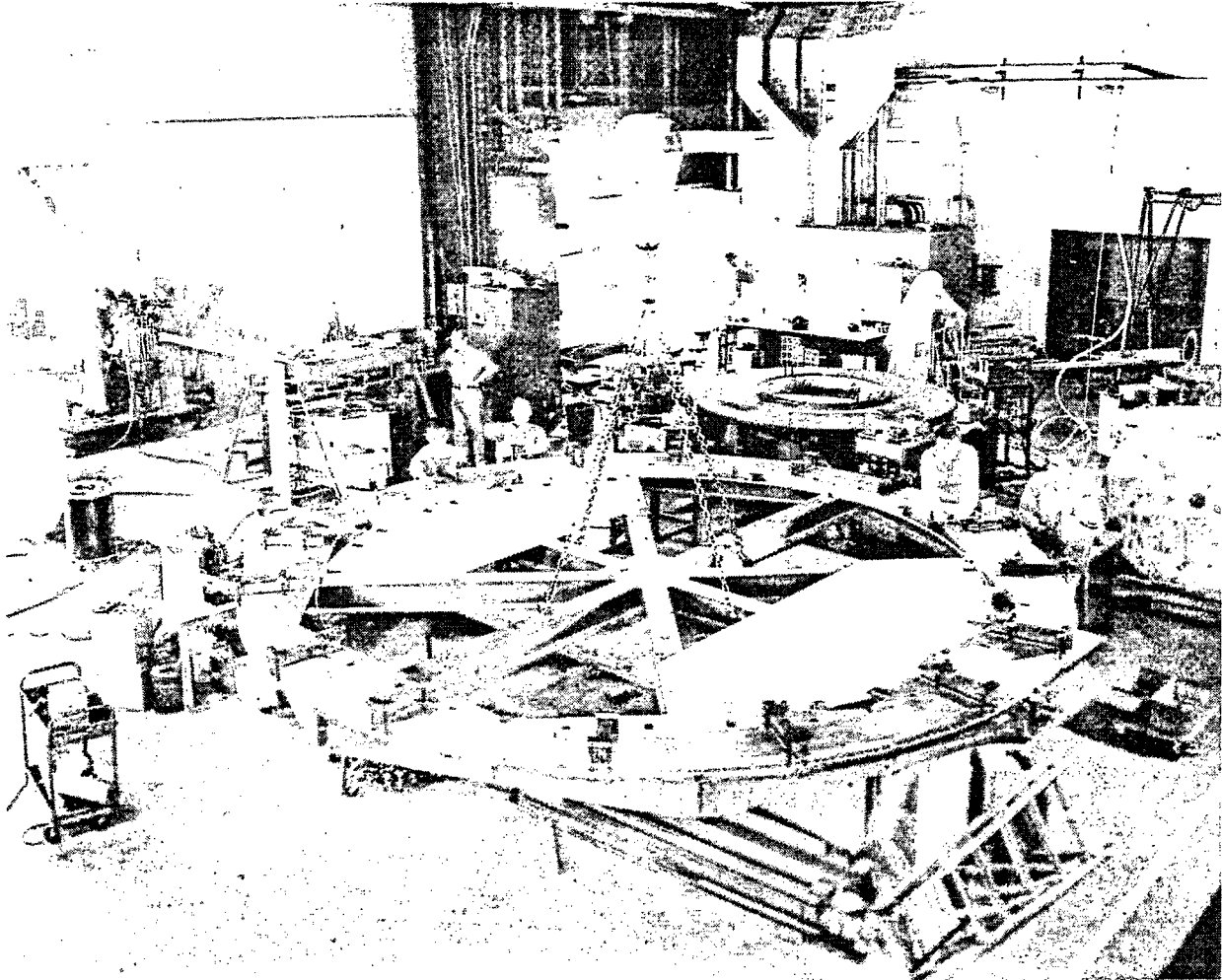


Fig. 10. A general view of the magnet winding facility showing a single pancake of the 1.8 T, 4.8 m i.d. bubble chamber coil in position on its winding jig.

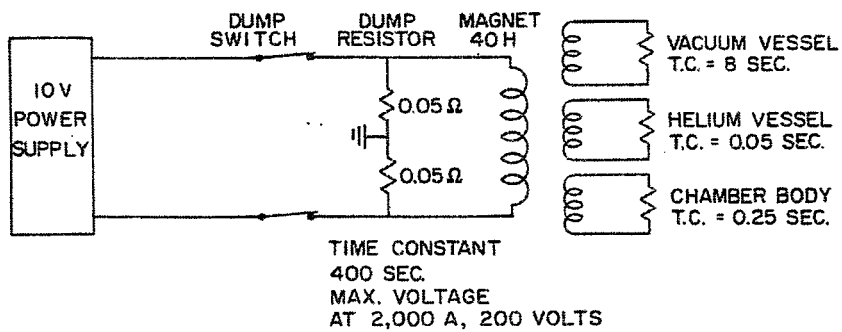


Fig. 11. Simplified diagram of the energizing and protective system for the large magnet system.

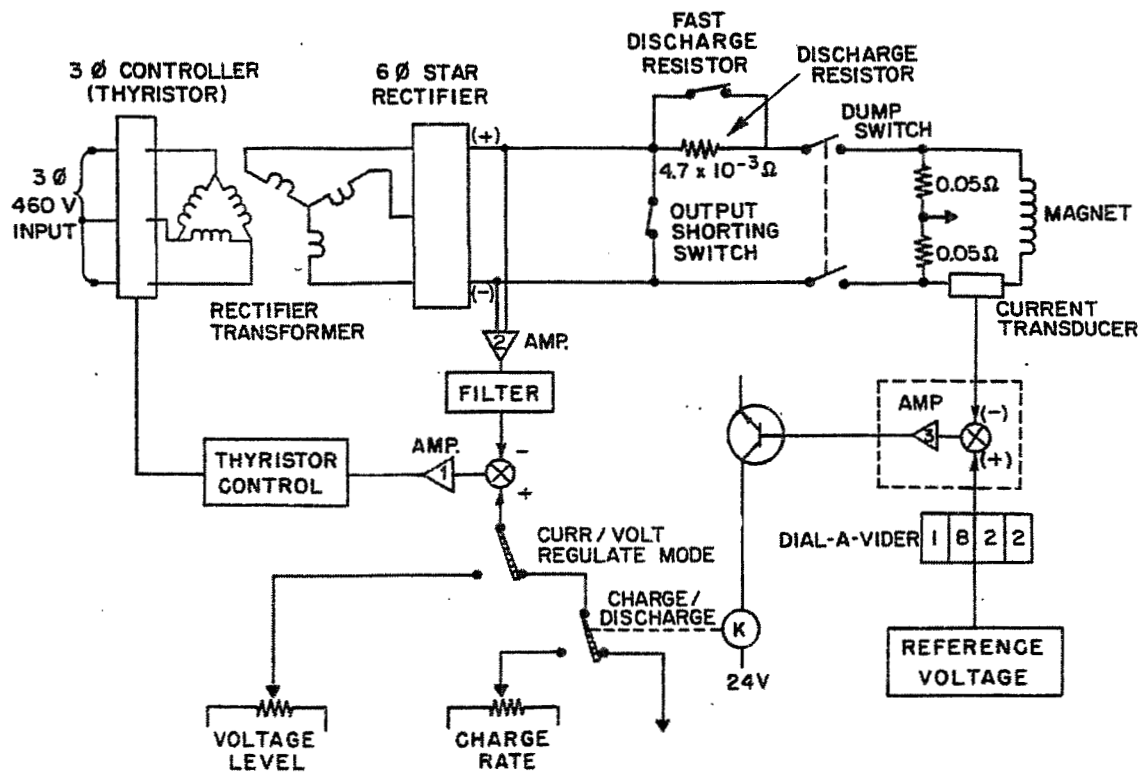


Fig. 12. Schematic circuit diagram of power supply.

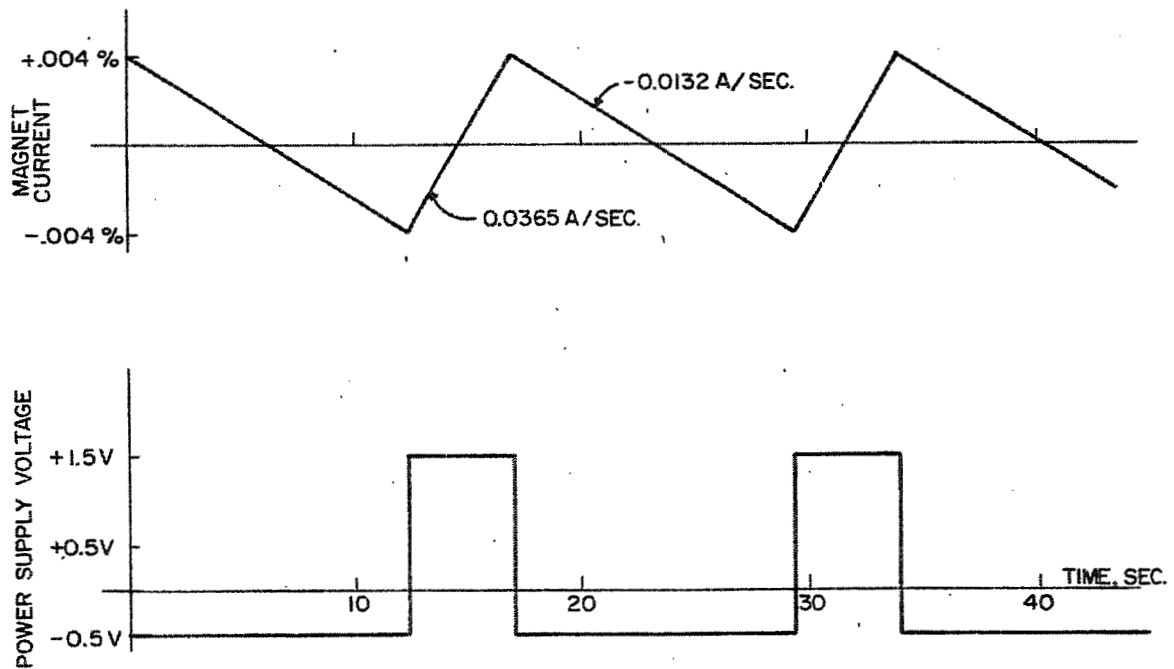


Fig. 13. Variation of coil current and on-off power supply voltage with time for normal magnet operation.